# Superconductivity of quasi-one-dimensional conductors in a high magnetic field

N. Dupuis and G. Montambaux
*Laboratoire de Physique des Solides, Université Paris-Sud, 91405 Orsay, France*
(Received 3 November 1993)

We determine the phase diagram of a quasi-one-dimensional superconductor (weakly coupled chains system with an open Fermi surface) in a magnetic field. A field $\mathbf{H}(0,H,0)$ along the $y$ direction (perpendicular the direction $x$ of highest conductivity) tends to confine the electronic motion in the $z$ direction. At low temperature, this effect cannot be neglected and the Ginzburg-Landau theory breaks down. We find that the usual Ginzburg-Landau regime is followed, when the field is increased, by a cascade of superconducting phases separated by first-order transitions, which ends with a strong reentrance of the superconducting phase where the chains interact by Josephson coupling. This high-field superconductivity can survive even in the presence of Pauli pair breaking because the quasi-one-dimensional Fermi surface allows one to construct a Larkin-Ovchinnikov-Fulde-Ferrell state that can exist far above the Pauli-limited field. Moreover, elastic scattering does not destroy the superconducting phases in clean materials with sufficiently large anisotropy. We show that the superconducting state evolves from an Abrikosov vortex lattice in weak field towards a Josephson vortex lattice in the reentrant phase. Between these two limits, the order parameter and the current distribution show laminar-type symmetry. The relevance of our results is discussed for quasi-one-dimensional organic superconductors and quasi-two-dimensional superconductors.

## I. INTRODUCTION

The microscopic justification[1] of the Ginzburg-Landau (GL) description of the mixed state of type-II superconductors[2] is based on a semiclassical approximation (known as the semiclassical phase integral or eikonal approximation) which completely neglects the quantum effects of the magnetic field.[3] At low temperature (or high magnetic field) and in sufficiently clean materials $\hbar\omega_c \gg k_B T, \hbar/\tau$ ($\omega_c$ being the characteristic magnetic frequency and $\tau$ the elastic scattering time) these effects cannot be neglected so that it is necessary to use an exact description of the magnetic field.

In isotropic superconductors with a closed Fermi surface, the magnetic field leads to Landau level quantization of the semiclassical orbits. Early studies of the influence of this quantization on the mixed state of type-II superconductors have shown that de Haas-van Alphen-like oscillations could occur in the superconducting transition temperature $T_c(H)$ in an external magnetic field.[4] More generally, the inclusion of Landau level quantization in the BCS theory leads to quantum oscillations in various physical quantities near $H_{c2}(0)$.[5] Experimental evidence for the importance of Landau quantization was found by Graebner and Robbins who observed de Haas-van Alphen oscillations in the mixed state of the layered dichalcogenide $2H$-$NbSe_2$.[6] Moreover it has been recently proposed by Tešanović, Rasolt, and Xing[7,8] that Landau level quantization can lead to reentrant behavior at a very high magnetic field ($\hbar\omega_c \gg E_F$): when only one Landau level is occupied, the orbital frustration of the order parameter disappears so that superconductivity is only limited by impurity scattering and a Pauli pair-breaking effect.[9] Unfortunately the very high fields needed restrict considerably the possible candidates and makes the experimental observation of this reentrant behavior a difficult challenge.

In quasi-one-dimensional (quasi-1D) conductors with an *open Fermi surface* such as can be found experimentally in weakly coupled chains systems, the magnetic field does not quantize the semiclassical orbits which are *open* but it induces a dimensional crossover.[10,11] This behavior is at the origin of a very rich variety of phenomena observed in organic quasi-one-dimensional conductors and in particular in the Bechgaard salts family: cascade of spin-density-wave phases appearing for increasing magnetic field, quantized Hall effect in a 3D conductor, etc.[12] The magnetic-field-induced dimensional crossover is expected to have also spectacular consequences on the phase diagram of a quasi-1D superconductor. This was first recognized by Lebed' who predicted a reentrant behavior of the superconductivity at a very high magnetic field in case of equal spin-triplet pairing.[13] It was noted by Lebed' that this reentrance should also be present (but at a lower temperature) in case of singlet pairing if the spatial dependence of the order parameter is correctly chosen: this property results from the quasi-1D geometry of the Fermi surface[14] which allows one to construct a Larkin-Ovchinnikov-Fulde-Ferrell (LOFF) state[15] which can exist far above the Shandrasekhar-Clogston (or Pauli) limit.[16] More recently, it has been shown that the theoretical phase diagram is richer that the one originally proposed by Lebed' and exhibits a cascade of first-order transitions between different supercon-

 

ducting phases with a new structure of the order parameter due to commensurability effects between the periodicity of the order parameter and the crystalline lattice spacing.[14]

In this paper, we present recent developments concerning the study of superconductivity at a high magnetic field in a quasi-1D conductor with the dispersion law ($\hbar = k_B = 1$ in the following and the Fermi energy is chosen as the origin of the energies):

$$E(\mathbf{k}) = v(|k_x| - k_F) + t_y \cos(k_y b) + t_z \cos(k_z c), \quad (1)$$

where $v$ is the Fermi velocity for the motion along the chains and $t_y$, $t_z$ are the coupling between chains separated by the distances $b, c$. The use of a linearized dispersion law is justified when $t_y$ and $t_z$ are much smaller than the Fermi energy. The magnetic field is assumed to be along the $y$ direction. We will consider both cases $T_c \ll t_z \ll t_y$ and $t_z \ll T_c \ll t_y$ where $T_c$ is the zero-field critical temperature. The former condition ensures that the smallest coherence length in the system is always much larger than the spacing between chains [$\xi_z(T) > \xi_z(0) \gg c$]. When quantum effects of the field are not taken into account, the discrete aspect of the system does not play an important role in this case: the superconductivity is well described by the anisotropic GL theory. The superconducting state is an anisotropic triangular Abrikosov vortex lattice, and the normal state is restored by the orbital effects of the field at $H_{c2}(T) = \phi_0/2\pi\xi_x(T)\xi_z(T)$ ($\phi_0$ is the flux quantum).[17] In the other case, when $t_z \ll T_c$, the chains interact by Josephson coupling at low temperature so that it is necessary to use the Lawrence-Doniach model[18] instead of the GL theory. The superconducting state is an anisotropic triangular lattice of Josephson vortices. At low temperature, vortices can fit between two chains so that the critical temperature becomes limited only by impurity scattering or the Pauli pair-breaking effect.[17]

As discussed in Ref. 14 a simple semiclassical analysis explains the origin of the reentrant behavior at a very high magnetic field. For a magnetic field $\mathbf{H}(0, H, 0)$ along the $y$ direction, the semiclassical electronic trajectories obtained from the equation of motion $d\mathbf{k}/dt = e\mathbf{v} \times \mathbf{k}$ are of the form $z = c(t_z/\omega_c)\cos(Gx)$, where $G = -eHc$ and $\omega_c = Gv$. The field reduces the amplitude of the electronic motion in the $z$ direction. At very high field ($\omega_c \gg t_z$), the amplitude of the trajectories becomes smaller than the distance between chains, showing that the electronic motion becomes localized in the $(x, y)$ planes. The magnetic field being parallel to the plane of the electronic motion, time-reversal symmetry is restored (if we ignore the Zeeman coupling) so that the orbital frustration of the order parameter vanishes [there is no magnetic flux through the 2D Cooper pairs located in the $(x, y)$ planes]. This magnetic-field-induced confinement is important only when the magnetic length $2\pi/G$ (the spatial periodicity of the semiclassical motion) is much smaller than the thermal length $v/2\pi T$ so that quantum effects can be ignored when $\omega_c \ll T$.

In the next section, we determine the transition temperature $T_c(H)$. Our calculation goes beyond the eikonal approximation and takes into account the quantum effects of the magnetic field. We first show that the BCS theory reduces to the Lawrence-Doniach model or to the anisotropic GL theory in the weak field limit where the eikonal approximation is justified. The transition line and the order parameter are then calculated numerically for any value of the field. It is shown that the phase diagram depends strongly on the ratio $t_z/T_c$. When $t_z/T_c$ decreases, the number of phases in the cascade of first-order transitions decreases and the critical temperature increases. For $t_z/T_c < 1$, the cascade disappears: the reentrant phase follows directly the semiclassical regime. The Pauli pair-breaking effect is discussed in detail. For a sufficiently small ratio $t_z/T_c$, the critical temperature of the LOFF state (for singlet superconductivity) can be in an experimentally accessible range for any value of the field. For larger values of this ratio, the cascade appears at a very low temperature and only the reentrant behavior is expected to be seen. We show that elastic scattering does not destroy the superconducting phases in clean materials with a sufficiently large anisotropy. We also show that the chains interact by Josephson coupling in the very high-field limit ($\omega_c \gg t_z$). Effects of fluctuations on the existence of a long-range order are briefly discussed. Finally, we present the evolution of the order parameter from the Abrikosov Gaussian solution in weak field towards an extended solution at high field.

In Sec. III, we determine the order parameter in the vicinity of $T_c(H)$. We follow the original approach proposed by Abrikosov[2,3] and write the order parameter as a linear combination of the solutions of the linearized gap equation. This linear combination is chosen in such a way that the order parameter describes an Abrikosov vortex lattice in weak field ($\omega_c \ll T$) and a Josephson vortex lattice at very high field ($\omega_c \gg t_z$). The current distribution is calculated in Sec. IV. At high field ($\omega_c \gg T$), the superconducting state differs qualitatively from the usual Abrikosov vortex lattice. In particular, the amplitude of the order parameter and the current distribution show a laminar structure.

In Sec. V, we discuss the case of the organic superconductors $(TMTSF)_2X$ where TMTSF=tetramethyl tetrathiafulvalene and $X = ClO_4$, $PF_6$. We briefly comment on the mechanisms which could be responsible for superconductivity in these materials and on the relevance of the model studied in Secs. II, III, and IV. We then discuss the expected phase diagram according to the value of $t_z$. In Sec. VI, we explain why the results obtained for a quasi-1D superconductor should also be valid for a quasi-2D superconductor at high parallel magnetic field and discuss the experimental consequences.

## II. TRANSITION LINE

In the absence of electron-electron interactions the system is described by the Hamiltonian $\mathcal{H}_0 = E(\mathbf{k} \to -i\nabla - e\mathbf{A})$ obtained from the dispersion law by the Peierls substitution. $\mathbf{A}$ is the magnetic vector potential. In the gauge $\mathbf{A}(0, 0, -Hx)$, the eigenstates and the corresponding eigenvalues are given by

$$\phi^{\alpha}_{\mathbf{k},\sigma}(x,l,m) = e^{ik_x x + ik_y bl + ik_z cm + i\alpha \frac{t_z}{\omega_c}\sin(k_z c - Gx)}, \quad (2)$$

$$\epsilon^{\alpha}_{\mathbf{k},\sigma} = v(\alpha k_x - k_F) + t_y \cos(k_y b) + \sigma \mu_B H, \quad (3)$$

where the integers $l$ and $m$ label the chains in the directions $y$ and $z$. $\sigma = +$ $(-)$ for $\uparrow$ $(\downarrow)$ spin and the $g$ factor is assumed to be equal to 2. Each eigenstate is labeled by the vector $\mathbf{k}$, where $k_y$ and $k_z$ are restricted to the first Brillouin zones $]-\pi/b, \pi/b]$ and $]-\pi/c, \pi/c]$ (note that $k_x$ is not the momentum). $\alpha = \mathrm{sgn}(k_x)$ refers to the left/right sheet of the Fermi surface. The confinement of the electrons in the $z$ direction appears only through the nondependence of $\epsilon^{\alpha}_{\mathbf{k},\sigma}$ on $k_z$. Using this latter property, it is possible to construct a set of eigenstates which are localized in the $z$ direction.[19] The real space one-particle Green's function also confirms the localized character of the electrons in the $z$ direction.[20] Taking advantage of the conservation of the transverse momenta $k_y$ and $k_z$ in the Landau gauge, we introduce a Green's function in the mixed representation $(x, k_y, k_z)$ by taking the Fourier transform with respect to $y$ and $z$:

$$\begin{aligned} G^{\alpha}_{\sigma}(x,x',k_y,k_z,\omega_n) &= e^{i\alpha \frac{t_z}{\omega_c}[\sin(k_z c - Gx) - \sin(k_z c - Gx')]} \sum_{k_x} e^{ik_x(x-x')} \tilde{G}^{\alpha}_{\sigma}(k_x,k_y,\omega_n) \\ &= \sum_{n,n'} \gamma^{\alpha}_{n}(k_z)\gamma^{\alpha}_{n'}(k_z)^* e^{-inGx + in'Gx'} \sum_{k_x} e^{ik_x(x-x')} \tilde{G}^{\alpha}_{\sigma}(k_x,k_y,\omega_n), \end{aligned} \quad (4)$$

where $\omega_n = 2\pi T(n+1/2)$ is a Matsubara frequency and $\tilde{G}^{\alpha}_{\sigma}(k_x,k_y,\omega_n)$ is the two-dimensional Green's function:

$$\begin{aligned} \tilde{G}^{\alpha}_{\sigma}(k_x,k_y,\omega_n) = [&i\omega_n - v(\alpha k_x - k_F) \\ &- t_y \cos(k_y b) - \sigma \mu_B H]^{-1}. \end{aligned} \quad (5)$$

The coefficients $\gamma^{\alpha}_{n}(k_z)$ come from the Fourier expansion of the periodic phase factor in (4):

$$\begin{aligned} \gamma^{\alpha}_{n}(k_z) &= \int_0^{2\pi} \frac{du}{2\pi} e^{inu + i\alpha \frac{t_z}{\omega_c}\sin(k_z c - u)} \\ &= e^{ink_z c} J_n\left(\alpha \frac{t_z}{\omega_c}\right), \end{aligned} \quad (6)$$

where $J_n$ is the $n$th-order Bessel function.

The attractive electron-electron interaction Hamiltonian is described by the BCS model with coupling parameter $\lambda > 0$:

$$\begin{aligned} \mathcal{H}_{\mathrm{int}} = -\frac{\lambda}{2} \sum_{\alpha,\alpha'=\pm,\sigma} bc \sum_{l,m} \int dx\, &\psi^{\alpha'\dagger}_{\sigma}(\mathbf{r}) \psi^{\overline{\alpha}'\dagger}_{\overline{\sigma}}(\mathbf{r}) \\ &\times \psi^{\overline{\alpha}}_{\overline{\sigma}}(\mathbf{r}) \psi^{\alpha}_{\sigma}(\mathbf{r}), \end{aligned} \quad (7)$$

where we note $\mathbf{r} = (x,l,m)$ and $\overline{\alpha} = -\alpha$, $\overline{\sigma} = -\sigma$. The $\psi^{\alpha}_{\sigma}(\mathbf{r})$'s are fermionic operators for particles moving on the sheet $\alpha$ of the Fermi surface. The interaction is effective only between particles whose energies are within $\Omega$ of the Fermi level.

We look for a BCS mean-field solution of the Hamiltonian $\mathcal{H}_0 + \mathcal{H}_{\mathrm{int}}$ with the order parameter

$$\Delta(\mathbf{r}) = \lambda\left[\langle \psi^{-}_{\uparrow}(\mathbf{r})\psi^{+}_{\downarrow}(\mathbf{r})\rangle - \langle \psi^{-}_{\downarrow}(\mathbf{r})\psi^{+}_{\uparrow}(\mathbf{r})\rangle\right] \quad (8)$$

corresponding to singlet-spin pairing. It is well known that 1D fluctuations cannot in principle be neglected in quasi-1D superconductors due to interferences between Cooper and Peierls channels at energies $\epsilon > t_y$ (or equivalently at length scales $< v/t_y$). However, in the "weak coupling limit" a mean-field (or ladder) approximation becomes correct below the one-particle dimensional crossover temperature where these two channels decouple, the effects of 1D fluctuations being then to renormalize the transverse bandwidths $t_y$ and $t_z$, and the coupling parameter $\lambda$.[21,22] In the following, the different parameters of the Hamiltonian have therefore to be understood as renormalized parameters. The transition line is determined by the linearized gap equation

$$\lambda^{-1}\Delta(x,q_z) = \int_{|x-x'|>d} dx' K(x,x',q_z)\Delta(x',q_z), \quad (9)$$

$$\begin{aligned} K(x,x',q_z) &= T\sum_{\omega_n} \sum_{\alpha,k_y,k_z} G^{\alpha}_{\uparrow}(x,x',k_y,k_z,\omega_n) G^{\overline{\alpha}}_{\downarrow}(x,x',-k_y,q_z-k_z,-\omega_n) \\ &= \frac{T}{bcv^2} \frac{\cos[2\mu_B H(x-x')/v]}{\sinh[|x-x'|2\pi T/v]} J_0\left(\frac{4t_z}{\omega_c}\sin\left[\frac{G}{2}(x-x')\right]\sin\left[q_z\frac{c}{2} - \frac{G}{2}(x+x')\right]\right). \end{aligned} \quad (10)$$

The cutoff $d$ is related to the energy $\Omega$. $\Delta(x,q_z)$ is the Fourier transform of the order parameter with respect to $z$. We have also used the fact that the highest $T_c(H)$ is obtained for a uniform order parameter along the field.

### A. Ginzburg-Landau regime ($\omega_c \ll T$)

In the weak field regime ($\omega_c \ll T$), the magnetic length $2\pi/G$ is much larger than the thermal length

$v/2\pi T$. Since $v/2\pi T$ acts as a cutoff, it is possible to replace $\sin[G(x-x')/2]$ by $G(x-x')/2$ in the kernel $K$ of the linearized gap equation. This approximation is strictly equivalent to the eikonal approximation[3] where the Green's functions are modified by the magnetic field only through the introduction of a phase factor equal to the circulation of the vector potential. The kernel $K$ is then given by

$$K^{(\mathrm{eik})}(x,x',q_z) = \frac{T}{bcv^2}\frac{\cos[2\mu_B H(x-x')/v]}{\sinh[|x-x'|2\pi T/v]} \times J_0\left(\frac{2t_z}{v}(x-x') \times \sin\left[q_z\frac{c}{2}-\frac{G}{2}(x+x')\right]\right). \quad (11)$$

The resulting integral equation can be converted into a second-order differential equation if we expand the gap $\Delta(x',q_z)$ and the argument of the Bessel function in second order in $x-x'$:

$$-v^2\frac{\partial^2\Delta}{\partial x^2} + t_z^2\left[1-\cos(q_z c - 2Gx)\right]\Delta = \frac{16\pi^2}{7\zeta(3)}T_c^2\left(1-\frac{T}{T_c}\right)\Delta, \quad (12)$$

where $\zeta(z)$ is Riemann's zeta function. This differential equation is very similar to the diffusion equation of the cooperon which has been previously studied in the context of Anderson localization[20] and can be justified in the same way.[23] Equation (12) is the linearized gap equation in the Lawrence-Doniach model.[18] When $T_c \ll t_z$, it can be further simplified by replacing the periodic potential in the lhs by a set of decoupled harmonic potentials located at points $q_z c/2G + n\pi/G$. A possible set of degenerate solutions corresponding to the highest $T_c(H)$ is defined by

$$\Delta_n(x,q_z) = f_0\left(x - \frac{q_z c}{2G} - n\frac{\pi}{G}\right), \quad (13)$$

where $f_0$ is a Gaussian function. The preceding result can be put in a more standard form by introducing the quantum number $q_z' = q_z + n2\pi/c$ (which varies between $-\infty$ and $\infty$). The solutions $\Delta(x,q_z')$ are then Gaussian functions centered at $q_z' c/2G = q_z'/2eH$. The critical temperature is given by

$$T_c(H) = T_c - \frac{7\sqrt{2}\zeta(3)}{16\pi^2}\frac{t_z\omega_c}{T_c}. \quad (14)$$

Thus in the weak field regime ($\omega_c \ll T$), quantum effects of the magnetic field can be ignored and the BCS theory reduces to the Lawrence-Doniach model or, when $T_c \ll t_z$, to the anisotropic GL theory.[24] Equation (12) is correct as long as the magnetic length $2\pi/G$ is much larger than the thermal length $v/2\pi T$. When $T_c \ll t_z$, we can use (14) to define a crossover temperature $T^*$ between a semiclassical GL regime and a quantum regime:

$$T^* \sim \frac{T_c}{1+\frac{7\sqrt{2}\zeta(3)t_z}{4T_c}}. \quad (15)$$

When $T_c \ll t_z$, $T^*$ is of the order of $T_c^2/t_z$. Contrary to the isotropic case where the crossover temperature is determined by the Fermi energy ($T^* \sim T_c^2/E_F$),[7] $T^*$ is determined by $t_z$ and can be in an experimentally accessible range if the anisotropy is large enough. This result is very important in view of the search for quantum effects near $H_{c2}^{(\mathrm{eik})}(0)$ (the upper critical field calculated in the eikonal approximation) and will be further discussed in the next section.

### B. Quantum regime ($\omega_c \gg T$)

In the quantum regime ($\omega_c \gg T$), the eikonal approximation for the Green's functions breaks down and one has to solve the integral equation (9) with the exact form of the kernel (10). $T_c(H)$ is clearly independent of $q_z$ (which only shifts the origin of the $x$ axis by $q_z c/2G$) allowing one to set $q_z = 0$. Using $K(x,x') = K(x+\pi/G, x'+\pi/G)$, the solution of (9) can be written without any loss of generality as a Bloch function:

$$\Delta_Q(x) = e^{iQx}\tilde{\Delta}_Q(x), \quad (16)$$

where $\tilde{\Delta}_Q(x)$ has the periodicity $\pi/G$ and $-G < Q \le G$. If we Fourier expand the periodic function $\tilde{\Delta}_Q(x)$,

$$\tilde{\Delta}_Q(x) = \sum_l \Delta_{2l}^Q e^{i2lGx}, \quad (17)$$

the linearized gap equation becomes a matrix equation for the coefficients $\Delta_{2l}^Q$:

$$\lambda^{-1}\Delta_{2l}^Q = \sum_{l'} A_{2l,2l'}^Q \Delta_{2l'}^Q, \quad (18)$$

$$A_{2l,2l'}^Q = \sum_N K_{N-2l,N-2l'}\tilde{K}(Q+NG). \quad (19)$$

$\tilde{K}(q_x)$ is the two-dimensional part of the kernel:

$$\tilde{K}(q_x) = T\sum_{\omega_n}\sum_{\alpha,k_x,k_y}\tilde{G}_\uparrow^\alpha(k_x,k_y,\omega_n) \times \tilde{G}_\downarrow^{\bar{\alpha}}(q_x-k_x,-k_y,-\omega_n) = \frac{c}{2}N(0)\sum_\alpha\left[\ln\left(\frac{2\Omega\gamma}{\pi T}\right) + \Psi\left(\frac{1}{2}\right) - \mathrm{Re}\,\Psi\left(\frac{1}{2}+\frac{\alpha v q_x + 2\mu_B H}{4i\pi T}\right)\right], \quad (20)$$

where $N(0) = 1/\pi vbc$ is the density of states per spin at the Fermi energy and $\gamma$ is the exponential of the Euler constant. $\Psi$ is the digamma function. The coefficients $K_{N_1,N_2}$ are defined by

$$K_{N_1,N_2} = \sum_{k_z,n_1,n_2} \gamma^+_{n_1}(k_z)\gamma^-_{N_1-n_1}(-k_z)\gamma^+_{n_2}(k_z)^* \times \gamma^-_{N_2-n_2}(-k_z)^* = \frac{1}{c} e^{i\frac{\pi}{2}(N_1-N_2)} \int_0^{2\pi} \frac{du}{2\pi} J_{N_1}\left(\frac{2t_z}{\omega_c}\sin(u)\right) \times J_{N_2}\left(\frac{2t_z}{\omega_c}\sin(u)\right). \quad (21)$$

The last expression is obtained using the definition (6) of the coefficients $\gamma^\alpha_n(k_z)$ where the Bessel functions are written as $J_n(z) = (2\pi)^{-1}\int_0^{2\pi} e^{inu - iz\sin(u)}du$.

We first consider the case without Pauli pair breaking. It then follows from (19) and (20) that the matrix elements $A^Q_{2l,2l'}$ present the usual logarithmic divergence $\tilde{K}(0) \sim \ln(2\Omega\gamma/\pi T)$ if $Q + NG$ can be equal to zero. Since $-G < Q \leq G$ this can be realized only for $Q = 0$ or $Q = G$. Therefore the highest $T_c(H)$ will be obtained for these two values of $Q$. The results of the numerical calculation of $T_c(H)$ are shown in Figs. 1–3 which correspond to different values of the ratio $t_z/T_c$. In the weak field regime ($\omega_c \ll T$), all the values of $Q$ between $-G$ and $G$ correspond to the same $T_c(H)$. In the quantum regime ($\omega_c \gg T$), this degeneracy is lifted: the highest $T_c(H)$ is always obtained for $Q = 0$ or $Q = G$ (in agreement with the preceding considerations), the last phase (very high field) corresponding to $Q = 0$. These two alternating solutions are characterized by a different structure of the order parameter. This means that successive phases are separated by first-order transitions. The phase diagram proposed by Lebed' corresponds to the solution $Q = 0$.[13] As can be seen from Figs. 1 and 2, the phase diagram depends strongly on the ratio $t_z/T_c$. When the anisotropy increases, the number of phases in the quantum regime decreases and the temperature in the low-temperature region increases in agreement with (15). When the Josephson limit is reached ($t_z \sim T_c$), the cascade of first-order transitions between the semiclassical regime and the reentrant phase disappears (Fig. 3).

We now consider the effect of Pauli pair-breaking by taking into account the Zeeman term. According to (19) and (20) the matrix elements $A_{2l,2l'}$ will present logarithmic divergences for $Q = \pm 2\mu_B H/v$ or $Q = \pm(G - 2\mu_B H/v)$. The shift $\pm 2\mu_B H/v$ of the value of $Q$ displaces the Fermi surfaces of spin $\uparrow$ and $\downarrow$ relative to each other and compensates partially the Pauli pair-breaking effect as is the case in a LOFF state[15] (note that the order parameter remains uniform along the magnetic-

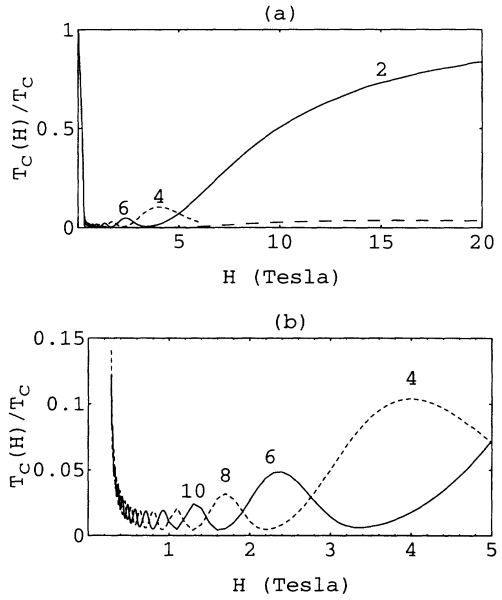


FIG. 1. Critical temperature $T_c(H)/T_c$ vs magnetic field ($t_z$ = 20 K and $T_c$ = 1.5 K). (a) The solutions $Q = 0$ (solid line) and $Q = G$ (dashed line) alternate for increasing magnetic field. Each phase is labeled by an even integer $N$ (see Sec. III). When the Pauli pair-breaking effect is taken into account $T_c(H)$ is strongly reduced but the reentrance at very high field is not suppressed (long-dashed line). (b) The low-temperature region in the absence of the Pauli pair-breaking effect.

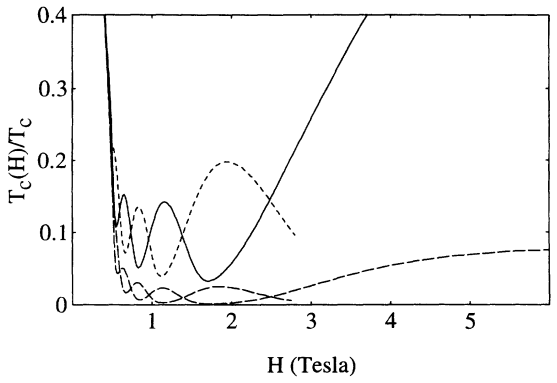


FIG. 2. Critical temperature $T_c(H)/T_c$ vs magnetic field ($t_z$ = 10 K and $T_c$ = 1.5 K). The solid (dashed) line corresponds to $Q = 0$ ($Q = G$) in the absence of the Pauli pair-breaking effect. The long-dashed lines correspond to the LOFF state.

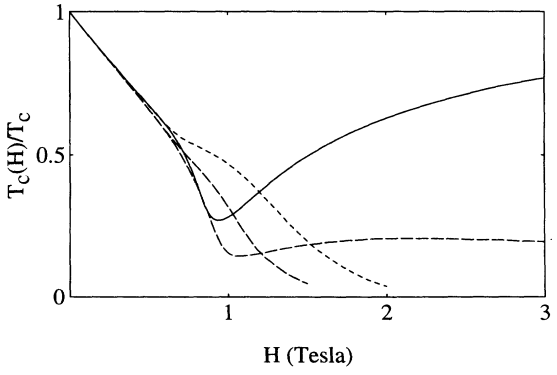


FIG. 3. Critical temperature $T_c(H)/T_c$ vs magnetic field near the Josephson limit ($t_z$ = 5 K and $T_c$ = 1.5 K). See the caption of Fig. 2 for the meaning of the different lines.

field direction). Since the logarithmic divergences survive for $\alpha = +$ or $\alpha = -$ in (20), one-half of the phase space is again available for pairing. The existence of a LOFF state (for every value of the field) is due to the quasi-1D structure of the Fermi surface. As can be seen from Figs. 1–3, the reentrance of the superconducting phase is not destroyed by the Pauli pair-breaking effect although $T_c(H)$ is considerably reduced compared with its value in the absence of Zeeman splitting. When the anisotropy is too small, the low-temperature region is destroyed by Pauli pair breaking as shown in Fig. 1 [in fact, the low-temperature region still exists but at a very low temperature (in the range of the mK) which cannot be seen in Fig. 1]. When the anisotropy is sufficiently large, the low-temperature region survives as can be seen in Figs. 2 and 3. In the Josephson limit ($t_z \sim T_c$), the last phase (very high field) corresponds to a slow decrease of $T_c(H)$ rather than to a real reentrant phase (Fig. 3): in this case, the transition between the semiclassical and quantum regimes is characterized by a sudden change in the slope of $T_c(H)$. It should be noted that the transition line obtained in the absence of Pauli pair breaking is not only of academic interest. For example, for triplet equal spin pairing, there is no effect of Zeeman splitting. The triplet state can be easily incorporated in the present theory if we describe the electron-electron interaction by two constants $g_1$ and $g_2$ corresponding to backward and forward scattering of two particles on opposite sides of the Fermi surface.[25] Then the singlet transition temperature corresponds to the one calculated in the presence of Pauli pair breaking with $\lambda = -(g_1 + g_2)/2$, while the triplet transition temperature corresponds to the one calculated in the absence of Pauli pair breaking with $\lambda = (g_1 - g_2)/2$. Moreover, most of the type-II superconductors are not Pauli limited and we expect that Pauli pair breaking will be inefficient close to $H_{c2}^{(\mathrm{eik})}(0)$ (obviously, our numerical calculations correspond to the Pauli limited case).

Before concluding on the possible existence of high-field superconductivity in quasi-1D conductors, it is necessary to consider the effect of impurity scattering. In a magnetic field, the superconducting state is not formed from time-reversal pairs and is expected to be sensitive to impurities. To leading order in $1/E_F\tau$ ($\tau$ being the elastic scattering time), impurity scattering is taken into account by including self-energy and vertex corrections into the kernel $K$ defined by (10).[26] Following such a procedure, we find that the effect of impurity scattering is weak, i.e., $|T_c^{\mathrm{dis}}(H) - T_c(H)| \ll T_c(H)$ where $T_c^{\mathrm{dis}}(H)$ is the critical temperature in the presence of disorder if[27]

$$\frac{\pi}{8\tau T_c(H)}(1-\bar{V}) \ll 1\,, \tag{22}$$

when Pauli pair breaking is not considered, and

$$\frac{\pi}{16\tau T_c(H)}\left[\left(1-\frac{\bar{V}}{2}\right)-\left(1+\frac{\bar{V}}{2}\right)\frac{T_c(H)^2}{\mu_B^2 H^2}\right] \ll 1\,, \tag{23}$$

for the LOFF state when Pauli pair breaking is taken into account. In the last equation, we assumed $T \ll \mu_B H$. In (22) and (23), $T_c(H)$ is the critical temperature calculated with and without Pauli pair breaking, respectively. We have introduced

$$\bar{V} = \frac{\ln(2\gamma\Omega/\pi T_c)}{\ln[2\gamma\Omega/\pi T_c(H)]}\,, \tag{24}$$

where $T_c(H)$ is the critical temperature without Pauli pair breaking. $\bar{V}$, which comes from vertex corrections in the linearized gap equation, tends to reduce the difference $T_c(H) - T_c^{\mathrm{dis}}(H)$. For the low-temperature regions ($T < \omega_c < t_z$) shown in Figs. 1(b) and 2, $\bar{V}$ is in the range 0.3–0.6 for a cutoff $\Omega$ in the range 30–300 K. According to (22), impurity scattering does not affect the critical temperature in the reentrant phase when Pauli pair breaking is neglected since $\bar{V} \to 1$ when $T_c(H) \to T_c$. This is a direct consequence of Anderson's theorem which states that the critical temperature is independent of a (weak) disorder for a system with time-reversal symmetry.[28] When the Zeeman term is taken into account, the reentrant phase becomes sensitive to the presence of disorder [Eq.(23)] since time-reversal symmetry is broken in this case whatever the value of the magnetic field. Obviously, inequalities (22) and (23) impose to consider clean superconducting materials with a critical temperature not too small. This latter condition will be an advantage to materials with a large anisotropy. To illustrate this point further, let us assume that $1/\tau \sim 100$ mK, a condition which is realized in the organic conductors $(TMTSF)_2ClO_4$ and $(TMTSF)_2PF_6$. Using inequalities (22) and (23) (which we rewrite as $\alpha \ll 1$, which defines $\alpha$), we can test the stability of the superconducting phase. For $T_c = 1.5$ K and $t_z = 5$ K (Fig. 3), the effect of disorder can be neglected. The reentrant phases shown in Figs. 1(a) and 2 are not destroyed by impurity scattering ($\alpha \ll 1$). On the other hand, the low-temperature region shown in Fig. 1(b) is likely to be affected by disorder since $\alpha \sim 0.5$–$0.75$. The low-temperature region of the LOFF state shown in Fig. 2 could also be affected by disorder since $\alpha \sim 0.55$–$0.6$. Thus, although inequalities (22) and (23) are quite restrictive, high-field superconductivity remains possible in clean materials which are sufficiently anisotropic.

The periodic part $\tilde{\Delta}_Q(x)$ of the order parameter is shown for increasing values of the magnetic field in Fig. 4 which corresponds to $T_c(H)$ shown in Fig. 1. In the GL regime, $\tilde{\Delta}_Q(x)$ is localized around the points $x_n = n\pi/G$. Using the degeneracy of $T_c(H)$ with respect to $Q$, it is possible to recover the Abrikosov Gaussian solution:

$$f_0(x - x_n) = \sum_Q e^{-iQx_n}\Delta_Q(x)\,. \tag{25}$$

In the quantum regime where the degeneracy of $T_c(H)$ with respect to $Q$ is lifted, $\tilde{\Delta}_Q(x)$ becomes extended. This suggests that the usual vortex lattice structure is strongly modified when $\omega_c \gg T$. At very high field ($\omega_c \gg t_z$), $\tilde{\Delta}_Q(x)$ becomes almost uniform.

The phase diagram shown in Figs. 1–3 can be explained qualitatively by a criterion of the type (we only consider the case $T_c \ll t_z$)

$$2\pi H\xi_x(T,H)\xi_z(T,H) \sim \phi_0\,, \tag{26}$$

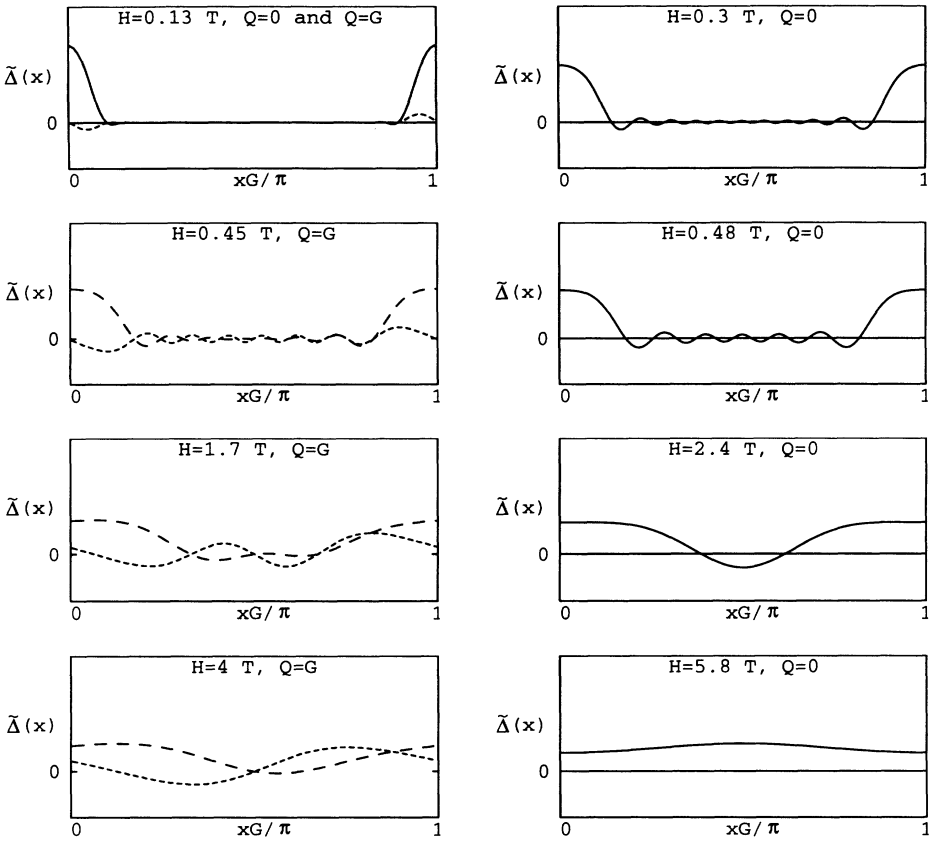


FIG. 4. Periodic part $\tilde{\Delta}_Q(x)$ of the order parameter for different values of the magnetic field. Solid line: $\tilde{\Delta}_{Q=0}(x)$ [$\tilde{\Delta}_{Q=0}(x)$ is real]. Dashed and long-dashed lines: real and imaginary parts of $\tilde{\Delta}_{Q=G}(x)$.

where $\xi_x(T,H)$ and $\xi_z(T,H)$ are characteristic lengths to be determined. In the GL regime $\xi_x(T,H) = \xi_x(T)$ and $\xi_z(T,H) = \xi_z(T)$ are the usual coherence lengths and we recover the result of the GL theory. In the quantum regime, these temperature dependent coherence lengths are not relevant any more and have to be replaced by magnetic-field dependent lengths: $\xi_x(T,H) = \xi_x(H)$ and $\xi_z(T,H) = \xi_z(H)$. According to the semiclassical analysis presented in the Introduction, we expect $\xi_x(H)$ to be roughly constant and $\xi_z(H)$ to decrease like $1/H$ by analogy with the transverse magnetic length $\sim c(t_z/\omega_c)$. $\xi_z(H)$ can be interpreted as the size of the Cooper pairs in the $z$ direction. The magnetic flux $H\xi_x(T,H)\xi_z(T,H)$ then becomes field independent: the dimensional crossover compensates the breakdown of time-reversal symmetry and freezes the orbital mechanism of destruction of the superconductivity. In this picture, the reentrant phase (very high field $\omega_c \gg t_z$) where the orbital frustration of the order parameter vanishes can be interpreted as the limit where the size of the Cooper pair in the $z$ direction becomes smaller than the spacing between chains: $\xi_z(T,H) \ll c$.

### C. Very high-field limit $\omega_c \gg t_z$

The relation $\xi_z(T,H) \ll c$ suggests that the chains interact by Josephson coupling when $\omega_c \gg t_z$. This becomes clear if we consider the linearized gap equation. In the very high-field limit, the hopping between chains is of order $t_z/\omega_c \ll 1$ and can be treated perturbatively. To first order in $(t_z/\omega_c)^2$, the linearized gap equation in real space is represented by the diagrams of Fig. 5. Figure 5(a) corresponds to the propagation of an electron-electron pair in the plane $z = mc$ and is the only contribution when the magnetic field is infinite. Figure 5(b) describes a finite extension of the Cooper pair in the $z$ direction [one of the electrons hops to the plane $z = (m \pm 1)c$ and comes back to the plane $z = mc$] and contribute to the reduction of the transition temperature. Figure 5(c) corresponds to the Josephson tunneling of a pair from the plane $z = mc$ to the plane $z = (m \pm 1)c$. This Josephson coupling results only from the magnetic-field-induced dimensional crossover and is realized when $\omega_c \gg t_z$, or equivalently $2\pi/G \ll r_J$ or $c(t_z/\omega_c) \ll c$ where $r_J = v/t_z$ is the Josephson length for the hopping in the $z$ direction. By analogy with the case of weakly coupled superconducting planes (the quantum effects of the magnetic field being neglected) where the minimum of the free energy corresponds to a triangular lattice of Josephson vortices at low temperature,[29] we expect that the superconducting state will also be a triangular lattice of Josephson vortices in this high-field limit $\omega_c \gg t_z$.

The linearized gap equation can be solved if we retain only terms of order $t_z^2/\omega_c^2$. We first consider the case without Pauli pair breaking. The coefficients $\Delta_{2l}^{Q=0} \equiv \Delta_{2l}$ are of higher order for $|2l| > 2$ and can be neglected. Noting that $\Delta_2 = \Delta_2^* = \Delta_{-2}$ and $A_{2,0}^{Q=0} \equiv A_{0,2} = A_{0,2}^*$, the linearized gap equation can be written as

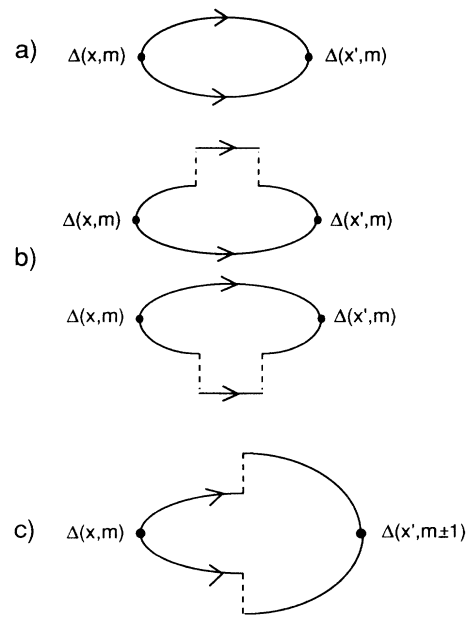


FIG. 5. Diagrammatic representation of the linearized gap equation to first order in $t_z^2/\omega_c^2$. The solid lines represent an electron propagating in a plane $z = mc$. The hopping between planes (of order $t_z/\omega_c$) is represented by dashed lines.

$$\begin{pmatrix} \lambda^{-1} - A_{0,0} & -2A_{0,2} \\ -A_{0,2} & \lambda^{-1} - A_{2,2} - A_{2,-2} \end{pmatrix} \begin{pmatrix} \Delta_0 \\ \Delta_2 \end{pmatrix} = \begin{pmatrix} 0 \\ 0 \end{pmatrix} . \tag{27}$$

To leading order in $t_z^2/\omega_c^2$, the coefficients $K_{N_1,N_2}$ are obtained by expanding the Bessel functions $J_n(z)$ in powers of $z$: $J_0(z) = 1 - z^2/4 + O(z^4)$, $J_{n\neq 0}(z) = (z/2)^n/n! + O(z^{n+2})$. One then obtains

$$\begin{aligned} A_{0,0} &= K_{0,0}\tilde{K}(0) + K_{1,1}[\tilde{K}(G) + \tilde{K}(-G)] , \\ A_{2,2} &= K_{0,0}\tilde{K}(2G) + K_{1,1}[\tilde{K}(G) + \tilde{K}(3G)] , \\ A_{0,2} &= K_{0,2}[\tilde{K}(0) + \tilde{K}(2G)] + K_{1,1}\tilde{K}(G) , \\ A_{2,-2} &= 0 , \end{aligned} \tag{28}$$

where

$$\begin{aligned} K_{0,0} &= \frac{1}{c}\left(1 - \frac{t_z^2}{\omega_c^2}\right) , \\ K_{1,1} &= \frac{t_z^2}{2c\omega_c^2} , \\ K_{0,2} &= -\frac{t_z^2}{4c\omega_c^2} . \end{aligned} \tag{29}$$

For $\omega_c \gg T$, the 2D susceptibilities $\tilde{K}(nG)$ are given by

$$\begin{aligned} \tilde{K}(0) &= cN(0)\ln\left(\frac{2\gamma\Omega}{\pi T}\right) , \\ \tilde{K}(nG) &= cN(0)\ln\left|\frac{2\Omega}{n\omega_c}\right| \quad \text{for } n \neq 0 . \end{aligned} \tag{30}$$

The critical temperature $T_c(H)$ is determined by

$$(\lambda^{-1} - A_{0,0})(\lambda^{-1} - A_{2,2}) - 2A_{0,2}^2 = 0 . \tag{31}$$

$A_{0,2}^2$ is of order $t_z^4/\omega_c^4$ and can be neglected. The highest critical temperature is then determined by $\lambda^{-1} - A_{0,0} = 0$. Using $\lambda^{-1} = N(0)\ln(2\gamma\Omega/\pi T_c)$, one obtains

$$T_c(H) = T_c\left(1 - \frac{t_z^2}{\omega_c^2}\ln\left|\frac{\gamma\omega_c}{\pi T_c}\right|\right) , \tag{32}$$

a result which agrees with the one derived by Burlachkov, Gor'kov, and Lebed'.[13] The relation between $\Delta_0$ and $\Delta_2$ is obtained from

$$-A_{0,2}\Delta_0 + (\lambda^{-1} - A_{2,2})\Delta_2 = 0 . \tag{33}$$

To leading order in $t_z^2/\omega_c^2$, one obtains

$$\Delta_2 \ln\left|\frac{2\gamma\omega_c}{\pi T}\right| = -\Delta_0 \frac{t_z^2}{4\omega_c^2}\ln\left|\frac{\gamma\omega_c}{2\pi T}\right| . \tag{34}$$

A similar procedure can be followed when Pauli pair breaking is considered. The only change is that $Q = 2\mu_B H/v$ is finite. When $\omega_c \gg T$, the 2D susceptibilities are given by

$$\begin{aligned} \tilde{K}(Q) &= \frac{c}{2}N(0)\ln\left|\frac{\gamma\Omega^2}{\pi T\mu_B H}\right| , \\ \tilde{K}(Q + nG) &= \frac{c}{2}N(0)\ln\left|\frac{4\Omega^2}{n\omega_c(4\mu_B H + n\omega_c)}\right| \quad \text{for } n \neq 0 , \end{aligned} \tag{35}$$

where we have assumed $|4\mu_B H + n\omega_c| \gg T$ in the last expression. We first calculate the critical temperature $T_c^{2D}(H)$ corresponding to isolated $(x,y)$ planes in the presence of Pauli pair breaking. This temperature is obtained from $\lambda^{-1} - c^{-1}\tilde{K}(Q) = 0$, which leads to

$$T_c^{2D}(H) = \frac{\pi T_c^2}{4\gamma\mu_B H} . \tag{36}$$

From $\lambda^{-1} - A_{0,0}^Q = 0$, we then obtain

$$\begin{aligned} T_c(H) = T_c^{2D}(H)\Bigg[1 - \frac{t_z^2}{\omega_c^2} \\ \times \ln\left(\frac{\gamma|\omega_c|}{\pi T_c^{2D}(H)}\sqrt{\left|1 - \frac{\omega_c^2}{16\mu_B^2 H^2}\right|}\right)\Bigg] . \end{aligned} \tag{37}$$

This expression is correct only for $|4\mu_B H \pm \omega_c| \gg T_c(H)$, a condition which will be verified in most cases at low temperature.

In this quasi-2D regime, it is necessary to consider the effect of thermodynamical fluctuations on the validity of the mean-field description. The problem of fluctuations is very similar to the one encountered in weakly coupled superconducting planes in parallel field described by the Lawrence-Doniach model: in the very high-field limit ($\omega_c \gg t_z$), our system can be viewed as a set of

anisotropic superconducting planes with a magnetic-field dependent Josephson coupling. Taking into account only the small (Gaussian) fluctuations of the phase of the order parameter, Efetov has shown that a strong parallel magnetic field suppresses long-range order in a set of weakly coupled planes described by the Lawrence-Doniach model: although the phase coherence between planes is absent, the superconductivity inside the planes survives (Kosterlitz-Thouless transition).[30] However a complete description should also take into account the role of topological excitations (vortices) (Ref. 17) and the electromagnetic coupling between planes[31] so that it is difficult to answer the question of the existence of a long-range order or of a Kosterlitz-Thouless transition.

## III. ORDER PARAMETER IN THE ORDERED PHASE

Following the original work of Abrikosov,[2,3] we write the order parameter for $T < T_c(H)$ as a linear combination of the solutions of the linearized gap equation. According to the preceding section, the order parameter evolves from a triangular Abrikosov vortex lattice in weak field $\omega_c \ll T$ (in this section we neglect the Zeeman splitting) to a triangular Josephson vortex lattice in very high field $\omega_c \gg t_z$. Consequently, it has to keep the same triangular symmetry throughout all the phase diagram. We therefore expect that it is possible to describe all the phase diagram with the same kind of linear combination. In the following we first construct the Abrikosov vortex lattice using the functions $\Delta_Q(x,q_z)$ introduced in the preceding section. We require the vortex lattice to have periodicity $a_z = Nc$ ($N$ integer) in the $z$ direction so that the vortex cores can lie between two planes (which will obviously minimize the free energy). $N$ has to be even in the case of a triangular lattice. We then show that the obtained solution can be naturally extended to the description of the quantum regime and in particular of the Josephson vortex lattice when $\omega_c \gg t_z$.

The order parameter describing the Abrikosov vortex lattice can be written as

$$\begin{aligned}\Delta(x,m) &= \sum_{q_z'=n_z'\frac{2\pi}{Nc}} C(n_z')e^{iq_z'c(m+a)} f_0\left(x-\frac{q_z'}{2eH}\right) \\ &= \sum_{n=-\infty}^{\infty}\sum_{q_z=n_z\frac{2\pi}{Nc}} C(n_z)e^{iq_z(m+a)+in2\pi a} \\ &\quad\times f_0\left(x-n\frac{\pi}{G}-\frac{q_zc}{2G}\right), \end{aligned} \tag{38}$$

where

$$C(n_z) = \begin{cases} C & \text{if } n_z \text{ is odd,} \\ iC & \text{if } n_z \text{ is even.}\end{cases} \tag{39}$$

$f_0$ is the Gaussian function introduced in the preceding section. $q_z' \in ]-\infty,\infty[$ is the momentum in an extended zone scheme. $q_z \in ]-\pi/c,\pi/c]$ is the momentum in a reduced zone scheme. The constant $a = 0$ (1/2) for $N/2$ odd (even) ensures that the vortex cores lie between two planes. Using relation (25) between $f_0$ and $\tilde{\Delta}_Q$ and restoring the $q_z$ dependence, we can write the order parameter as

$$\begin{aligned}\Delta(x,m) = \sum_Q \sum_{q_z=n_z\frac{2\pi}{Nc}} \sum_{n=-\infty}^{\infty} C(n_z)e^{in2\pi(a-\frac{Q}{2G})+iq_zc(m+a)} \\ \times\Delta_Q(x,q_z)\,. \end{aligned} \tag{40}$$

After summation over $n$, only the contribution $Q = 0$ ($Q = G$) for $N/2$ odd (even) subsists:

$$\begin{aligned}\Delta_{Q,N}(x,m) &= \sum_{q_z=n_z\frac{2\pi}{Nc}} C(n_z)e^{in_z\frac{\pi Q}{NG}}\Delta_Q(x,q_z)e^{iq_zcm} \\ &= C\sum_l \Delta_{2l}^Q e^{i(Q+2lG)x} \\ &\quad\times\sum_{p=-\infty}^{\infty}\left[1-i(-1)^p\right]\delta_{l-m,p\frac{N}{2}}\,. \end{aligned} \tag{41}$$

In deriving (40) and (41), we have included some numerical factors in the constant $C$. Thus we eventually come to the important result that the Abrikosov vortex lattice with periodicity $a_z = Nc$ can be constructed only with $\Delta_{Q=0}$ and $\Delta_{Q=G}$, the value of $Q$ depending on the parity of $N/2$. Solution (41) is naturally extended to the quantum regime where the best solutions also correspond to $Q = 0$ and $Q = G$. As will be shown latter, it describes correctly the Josephson vortex lattice in the limit $\omega_c \gg t_z$. It can be seen that $|\Delta_{Q,N}(x,m)|$ has periodicity $a_x = 2\pi/NG$ in the $x$ direction. We have the usual relation $Ha_xa_z = 2\phi_0$ showing that there are two flux quanta in the unit cell $(a_x,a_z)$ (which contains two vortices in the GL regime).

In order to know completely the order parameter, we have to determine the value of $N$. In the GL regime, the periodicity is given by the coherence lengths. We have $a_x/a_z = \sqrt{3}\xi_x/\xi_z = \sqrt{3}\Gamma$ where $\Gamma = v\sqrt{2}/t_zc$ is the anisotropy factor, which leads to

$$N_{\mathrm{GL}} \sim \sqrt{\frac{2\pi t_z}{\sqrt{6}\omega_c}}\,. \tag{42}$$

In the quantum regime, we assume that each phase transition when the field is increased corresponds to a decrease of $N$ by two units, the last phase (Josephson vortex lattice) corresponding to $N = 2$. The cascade of phase transitions is then due to commensurability effects between the crystalline lattice spacing $c$ and the periodicity $a_z$ of the order parameter. As in the GL regime, the phases $Q = 0$ ($Q = G$) correspond to $N/2$ odd (even). Using the fact that the maxima in $T_c(H)$ are determined by the extrema of $J_0(4t_z/\omega_c)$, we obtain

$$N_{\mathrm{QR}} \sim \frac{3}{2} + \frac{8t_z}{\pi\omega_c}\,. \tag{43}$$

The periodicity $a_z = Nc$ is not determined by the coherence length anymore but by the transverse magnetic length $\sim c(t_z/\omega_c)$. This result has to be compared with the case of isotropic superconductors where the size of the vortex lattice in high field is determined by the magnetic length $1/\sqrt{eH}$.[7] Since $N \sim 1/H$, $a_x$ is roughly a constant function of the field. It is interesting to note

that the characteristic length $a_x$ appears in the linearized gap equation. As can be seen from Fig. 4, the number of nodes in $\tilde{\Delta}_{Q=0}(x)$ is equal to $N_{\rm QR}/2-1$ [the same kind of observation can be made for $\Delta_{Q=G}(x)$]. $a_x = 2\pi/N_{\rm QR}G$ is then the mean distance between two nodes.

The transition between the GL regime and quantum regime is reached for $2\pi/G \sim v/2\pi T$. When $T_c \ll t_z$, the corresponding periodicities are given by

$$N_{\rm GL}^{(0)} \sim \frac{t_z}{T_c}\sqrt{\frac{7\zeta(3)}{8\sqrt{3}\pi}}\,,$$
$$N_{\rm QR}^{(0)} \sim \frac{3}{2} + \frac{t_z^2}{T_c^2}\frac{7\sqrt{2}\zeta(3)}{2\pi^3}\,. \qquad (44)$$

When $T_c \ll t_z$, we always have $N_{\rm GL}^{(0)} \ll N_{\rm QR}^{(0)}$. $N$ cannot be a monotonic decreasing function of the field but has to increase strongly at the transition between the GL and quantum regimes. With the parameters used to obtain Fig. 1, $N_{\rm GL} \sim 6$ at the end of the GL regime, while it is possible to distinguish 21 phases in the quantum regime. This increase of $N$ corresponds to a change in the structure of the order parameter as will be shown below. Close to the Josephson limit $T_c \sim t_z$, the cascade of phase transitions disappears and we have $N_{\rm GL}^{(0)} \sim N_{\rm QR}^{(0)} \sim 2$.

Before representing graphically the order parameter, we calculate the current distribution. We also show that the order parameter defined by (41) corresponds to a Josephson vortex lattice when $\omega_c \gg t_z$.

## IV. CURRENT DISTRIBUTION IN THE ORDERED PHASE

### A. General expressions

Once the order parameter is known, we can calculate the correction to the Green's function to lowest order (in the intermediate calculations, we do not take into account the $y$ direction which does not play any role):

$$\delta G_\sigma^\alpha(x,m;x',m',\omega_n) = -c^2 \sum_{m_1,m_2}\int dx_1\,dx_2\, G_\sigma^\alpha(x,m;x_1,m_1,\omega_n)\Delta_{Q,N}(x_1,m_1)$$
$$\times G_{\overline{\sigma}}^{\overline{\alpha}}(x_2,m_2;x_1,m_1,-\omega_n)\Delta_{Q,N}^*(x_2,m_2)G_\sigma^\alpha(x_2,m_2;x',m',\omega_n)\,, \qquad (45)$$

and the current distribution

$$j_x(x,m) = ev\sum_\alpha \alpha T\sum_{\omega_n,\sigma}\delta G_\sigma^\alpha(x,m;x,m,\omega_n)\,,$$
$$j_z(x,m,m+1) = -\frac{et_z c}{2i}\left[e^{c\partial_z - iGx} - e^{c\partial_{z'}+iGx'}\right]T\sum_{\omega_n,\sigma,\alpha}\delta G_\sigma^\alpha(x,m;x',m',\omega_n)|_{x=x',m=m'}\,. \qquad (46)$$

Here $j_z(x,m,m+1)$ is the current at point $x$ between the chains $m$ and $m+1$. In the GL regime, these expressions can be approximated by the ones obtained in the Lawrence-Doniach model as Eq. (9) could be approximated by Eq. (12) in the preceding section:

$$j_x(x,m) = \frac{7\zeta(3)}{8\pi^3T^2}\frac{ev}{bc}\left[i\Delta_{Q,N}(x,m)\partial_x\Delta_{Q,N}^*(x,m) + \text{c.c.}\right],$$
$$j_z(x,m,m+1) = \frac{7\zeta(3)}{8\pi^3T^2}\frac{et_z\sqrt{2}}{bc}|\Delta_{Q,N}(x,m)\Delta_{Q,N}(x,m+1)|\sin[\varphi_{Q,N}(x,m+1) - \varphi_{Q,N}(x,m) - 2Gx]\,, \qquad (47)$$

where $\varphi_{Q,N}(x,m)$ is the phase of $\Delta_{Q,N}(x,m)$. In the quantum regime ($\omega_c \gg T$), a somewhat lengthy calculation leads to the following expressions for the Fourier transform $\mathbf{j}(q_x = pNG, q_z = P2\pi/Nc)$ ($P = 1,...,N$ and $p$ are integers) of the current:[32]

$$j_x(p,P) = -\frac{8e}{Nbc}\sum_{N_1,N_1'}\sum_{N_2,N_2'}\Delta_{N_1'}^Q\Delta_{N_2'}^{Q*}F_{N_1+N_1',N_2+N_2'}e^{-i(N_2+N_2')\frac{P\pi}{N}}$$
$$\times e^{i\frac{\pi}{2}(pN-N_1'+N_2')}J_{pN-N_1'-N_1+N_2'+N_2}\left(2\frac{t_z}{\omega_c}\sin P\frac{\pi}{N}\right)$$
$$\times\left\langle e^{-i(pN-N_1'-N_1+N_2'+N_2)u}J_{N_1}\left(-2\frac{t_z}{\omega_c}\sin\left[u+P\frac{\pi}{N}\right]\right)J_{N_2}\left(-2\frac{t_z}{\omega_c}\sin(u)\right)\right\rangle_u \eta_{p,P}\,, \qquad (48)$$

and

$$j_z(p,P) = \frac{4et_z}{iNvb}\sum_{\beta=\pm}\beta\sum_{N_1,N_1'}\sum_{N_2,N_2'}\Delta^{Q}_{N_1'}\Delta^{Q*}_{N_2'}F_{N_1+N_1',N_2+N_2'}e^{-i(N_2+N_2'-1)\frac{P\pi}{N}}$$

$$\times e^{i\frac{\pi}{2}(pN-N_1'+N_2'+\beta)}J_{pN-N_1'-N_1+N_2'+N_2+\beta}\left(2\frac{t_z}{\omega_c}\sin P\frac{\pi}{N}\right)$$

$$\times\left\langle e^{-i(pN-N_1'-N_1+N_2'+N_2)u}J_{N_1}\left(-2\frac{t_z}{\omega_c}\sin\left[u+P\frac{\pi}{N}\right]\right)J_{N_2}\left(-2\frac{t_z}{\omega_c}\sin(u)\right)\right\rangle_u \eta_{p,P}\,, \tag{49}$$

where we use the notation $< \cdots >_u = \int_0^{2\pi}\cdots\frac{du}{2\pi}$. The constant $C$ appearing in (41) has been set equal to 1. The functions $F_{N,M}$ and $\eta_{p,P}$ are defined by

$$F_{N,M} = \begin{cases} 0 & \text{if } x = y = 0\,, \\ \frac{1}{\pi x} & \text{if } x = y\ (\neq 0)\ , \\ \frac{1}{\pi y}\ln\left|\frac{y\gamma}{\pi T}\right| & \text{if } x = 0 \text{ and } y \neq 0\ , \\ \frac{1}{\pi x}\ln\left|\frac{x\gamma}{\pi T}\right| & \text{if } y = 0 \text{ and } x \neq 0\ , \\ \frac{1}{\pi(y-x)}\ln\left|\frac{y}{x}\right| & \text{if } x \neq y \text{ and } x, y \neq 0, \end{cases} \tag{50}$$

where $x = -N\omega_c - vQ$ and $y = -M\omega_c - vQ$, and

$$\eta_{p,P} = \begin{cases} 1 & \text{if } p \text{ and } P \text{ are even}, \\ i & \text{if } p \text{ and } P \text{ are odd}, \\ 0 & \text{otherwise.} \end{cases} \tag{51}$$

The general expressions (41), (48), and (49) of the order parameter and the current distribution can be calculated numerically for any value of the magnetic field. The order parameter and the current distribution are shown in Fig. 6 for a weak magnetic field ($\omega_c \ll T$) [Figs. 6–10 correspond to $T_c(H)$ shown in Fig. 1]. $\Delta_{Q,N}(x,m)$ is obtained from (41) and $N$ is determined by (42). The current distribution is obtained from (47). The superconducting state is a triangular Abrikosov vortex lattice.

In the high-field limit $\omega_c \gg T$, the order parameter and the current distribution are shown in Figs. 7–10. The periodicity $N$ is obtained from (43) and the current distribution is given by (48) and (49). The superconducting state differs qualitatively from the Abrikosov vortex lattice shown in Fig. 6. The amplitude of $\Delta_{Q,N}(x,m)$ and the current distribution show a symmetry of laminar type consistent with the localized character of the electronic motion in the $z$ direction. An important aspect of the superconducting state in the quantum regime is that each chain carries a nonzero total current (except in the last phase). As shown in Fig. 10, the last phase ($N = 2$) corresponds to a Josephson vortex lattice.

### B. Very high-field limit $\omega_c \gg t_z$

The general expressions for the order parameter and the current distribution can be simplified in the very high-field limit $\omega_c \gg t_z$ if we retain only terms of order $t_z^2/\omega_c^2$. The order parameter is given by

$$\Delta_{Q=0,N=2}(x,m) = \Delta_0[1 - i(-1)^m] + 2\Delta_2\cos(2Gx)[1 + i(-1)^m]\,. \tag{52}$$

In order to obtain the expression of the current to leading order in $t_z^2/\omega_c^2$, we have to expand the Bessel functions appearing in (48) and (49) with respect to $t_z^2/\omega_c^2$. The different contributions to $j_x(p,P)$ are

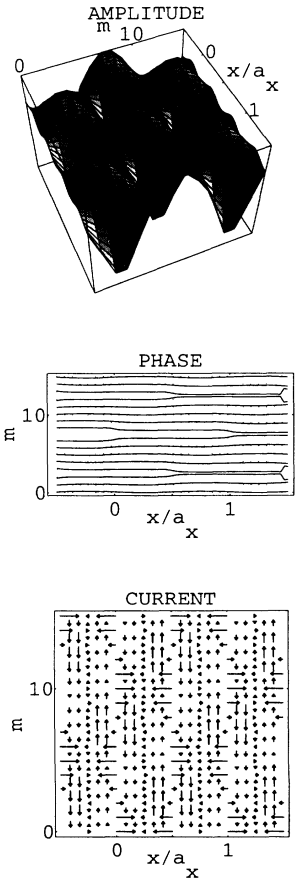


FIG. 6. Phase $Q = 0$, $N = 10$ ($H = 0.13$ T). On the middle figure, the distance between two horizontal dotted lines corresponds to $2.5\pi$.

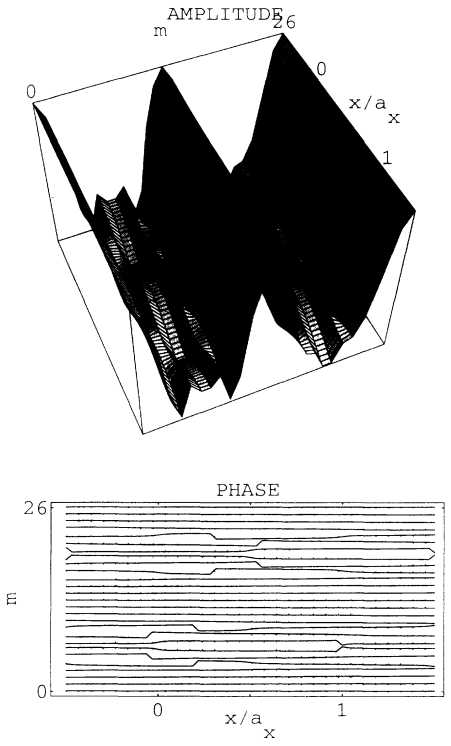


FIG. 7. Phase $Q = 0$, $N = 26$ ($H = 0.48$ T).

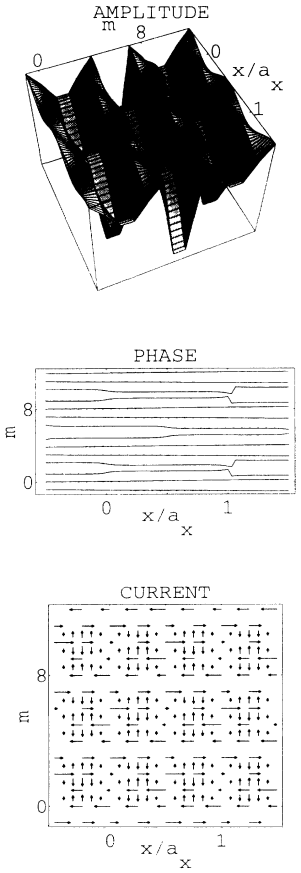


FIG. 8. Phase $Q = G$, $N = 8$ ($H = 1.7$ T).

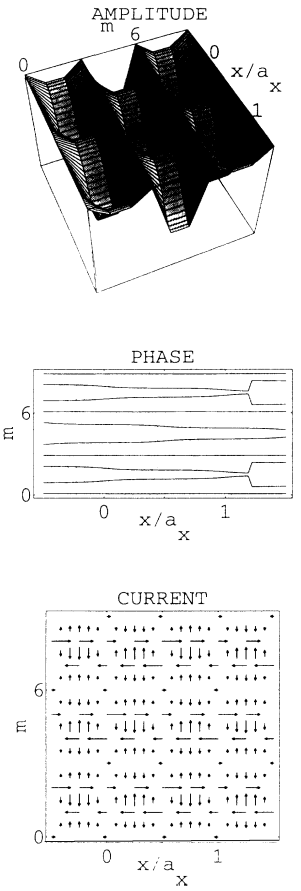


FIG. 9. Phase $Q = 0$, $N = 6$ ($H = 2.4$ T).

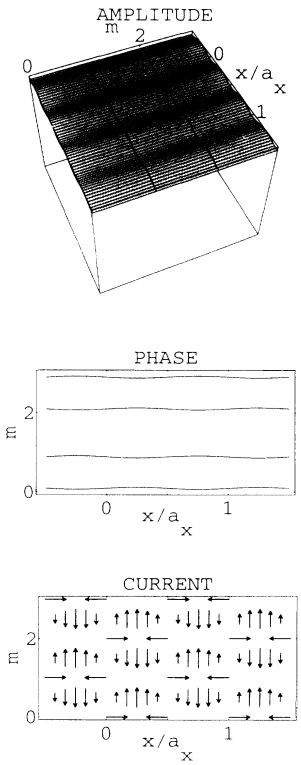


FIG. 10. Phase $Q = 0$, $N = 2$ ($H = 5.8$ T).

$$N_1' = 2p,\ N_1 = N_2 = N_2' = 0 \rightarrow j_x^{(1)}(p,1) = -4ip\frac{e}{bc}\Delta_0\Delta_2 F_{2,0}\,,$$

$$N_2' = 2p,\ N_1 = N_2 = N_1' = 0 \rightarrow j_x^{(2)}(p,1) = -4ip\frac{e}{bc}\Delta_0\Delta_2 F_{2,0}\,,$$

$$N_1 = 2p,\ N_2 = N_1' = N_2' = 0 \rightarrow j_x^{(3)}(p,1) = ip\frac{e}{bc}\frac{t_z^2}{\omega_c^2}\Delta_0^2 F_{2,0}\,,$$

$$N_2 = 2p,\ N_1 = N_1' = N_2' = 0 \rightarrow j_x^{(4)}(p,1) = ip\frac{e}{bc}\frac{t_z^2}{\omega_c^2}\Delta_0^2 F_{2,0}\,,$$

$$N_1 = p,\ N_2 = N_1' = N_2' = 0 \rightarrow j_x^{(5)}(p,1) = -2ip\frac{e}{bc}\frac{t_z^2}{\omega_c^2}\Delta_0^2 F_{1,0}\,,$$

$$N_2 = p,\ N_1 = N_1' = N_2' = 0 \rightarrow j_x^{(6)}(p,1) = -2ip\frac{e}{bc}\frac{t_z^2}{\omega_c^2}\Delta_0^2 F_{1,0}\,, \tag{53}$$

where $p = \pm 1$. The total contribution is given by

$$j_x(p,1) = -ip\frac{8e}{bc}\left[\Delta_0\Delta_2 F_{2,0} - \Delta_0^2\frac{t_z^2}{4\omega_c^2}F_{2,0} + \Delta_0^2\frac{t_z^2}{2\omega_c^2}F_{1,0}\right]. \tag{54}$$

Using the definition of $F_{1,0}$, $F_{2,0}$ and relation (34) between $\Delta_0$ and $\Delta_2$, the preceding expression is written as

$$j_x(p,1) = 4ipeN(0)G^{-1}\frac{t_z^2}{2\omega_c^2}\Delta_0^2\ln\left|\frac{\gamma\omega_c}{\pi T}\right|. \tag{55}$$

The current along the chains is then given by

$$j_x(x,m) = -4eN(0)G^{-1}\frac{t_z^2}{\omega_c^2}\Delta_0^2\ln\left|\frac{\gamma\omega_c}{\pi T}\right|(-1)^m\sin(2Gx)\,. \tag{56}$$

The different contributions to $j_z(p,P)$ are

$$N_1 = p,\ N_2 = N_1' = N_2' = 0 \rightarrow j_z^{(1)}(p,1) = -\frac{et_z^2}{vb\omega_c}\Delta_0^2 F_{1,0}\,,$$

$$N_2 = p,\ N_1 = N_1' = N_2' = 0 \rightarrow j_z^{(2)}(p,1) = -\frac{et_z^2}{vb\omega_c}\Delta_0^2 F_{1,0}\,, \tag{57}$$

where $p = \pm 1$. The total contribution is then given by

$$j_z(p,1) = 2eN(0)c\frac{t_z^2}{\omega_c^2}\Delta_0^2\ln\left|\frac{\gamma\omega_c}{\pi T}\right|, \tag{58}$$

from which we deduce

$$j_z(x,m) = 4eN(0)c\frac{t_z^2}{\omega_c^2}\Delta_0^2\ln\left|\frac{\gamma\omega_c}{\pi T}\right|(-1)^m\cos(2Gx)\,. \tag{59}$$

Equations (52), (56), and (59) are characteristic of a triangular lattice of Josephson vortices.

## V. BECHGAARD SALTS AT HIGH MAGNETIC FIELD

The phase diagram of the Bechgaard salts $(TMTSF)_2X$ (where $X = ClO_4, PF_6$) has the unique feature that it presents three different ground states [metallic, superconducting, and spin-density wave (SDW)] as a function of pressure and magnetic field.[33] A great deal of theoretical effort has been devoted to an explanation of this phase diagram based on the $g$-ology model.[22,34] Many of the data observed in these materials seem to show that the intrachain interactions are repulsive and indicate that the superconductivity is not of conventional type: the sensitivity of the superconducting critical temperature to pressure, the existence of antiferromagnetic fluctuations above this temperature, the existence of a cascade of magnetic-field-induced SDW phases well described in the repulsive Hubbard model by a mean-field theory ("standard model") (see Refs. 22 and 34 for a more detailed discussion). Although different mechanisms have been proposed, such as for example exchange of spin fluctuations[35] or coherent tunneling of correlated pairs of particles,[36] the problem of the origin of the superconductivity in these salts has not received a definite answer yet.

Whatever the mechanism responsible for superconductivity in the Bechgaard salts, the theory we have developed in the preceding sections (which assumes attractive intrachain interactions) is probably not the right starting point in the case of the Bechgaard salts.[37] However, we claim that our results are valid (at least from a qualitative point of view) independently of the microscopic origin of the superconductivity. The existence of superconductivity at high magnetic field in a quasi-1D superconductor is due only to the magnetic-field-induced dimensional crossover and does not rely on a particular model of su-

perconductivity. This is, for example, obvious for the reentrant phase which results from the 2D localization of the one-particle quantum states. We therefore expect that the phase diagrams shown in Figs. 1–3 are qualitatively correct in the case of the Bechgaard salts.

The alignment of the field along the $y$ direction is crucial in the case of the Bechgaard salts. First the value of $t_y$ is much too large to see any quantum effects, at realistic values of temperature and field, for a magnetic field along the $z$ direction. Moreover, a field in the $z$ direction would induce a cascade of SDW phases which would prevent the existence of a superconducting phase at high magnetic field. For a field along the $y$ direction, this situation does not occur because the deviation to the perfect nesting in the $y$ direction, which is not affected by the field, is large enough to suppress the SDW phases. Let us also mention that there is no contradiction between the absence of electron-hole nesting and the possibility to construct a LOFF state. For example the electron-hole nesting is destroyed by the additional term $t'_y \cos(2k_y b)$ in the dispersion law $E(\mathbf{k})$ describing second-neighbor interaction between chains. On the other hand, this additional term does not affect the LOFF state which can be constructed as long as the use of a linearized dispersion law is justified, independently of its electron-hole nesting properties. It should be also noted that a precise alignment of the field along the $y$ direction is required. A component of the field $H_x$ or $H_z$ along the $x$ or $z$ directions would create an additional flux through the Cooper pairs and decrease the critical temperature $T_c(H)$. The effect of a nonzero $H_x$ or $H_z$ will be small if $H_x \ll H_{c2}^x(0)$ and $H_z \ll H_{c2}^z(0)$, where $H_{c2}^x(0)$ and $H_{c2}^z(0)$ are the critical fields calculated in the eikonal approximation. Since $H_{c2}^z(0) \ll H_{c2}^x(0)$, the strongest constraint comes from the component $H_z$. For a field $H \sim 10$ T, using $H_{c2}^z(0) \sim 0.02$ T,[38] we obtain $\Delta\theta \sim H_z/H \ll 1°$. In the case of a triclinic structure (which is the case in the Bechgaard salts), the field has to be along the $b'$ axis, which is in the most conducting plane and perpendicular to the chains axis. This will ensure that $H_x = H_z = 0$.

The expected phase diagram depends strongly on the ratio $t_z/T_c$. There are two different opinions in the literature concerning the value of $t_z$. According to many authors, $t_b = t_y/2$ and $t_c = t_z/2$ are in the ranges 200–300 K, and 5–10 K, respectively, which corresponds to Figs. 1 and 2. With these values of $t_c$, the reentrant behavior and also the cascade if $t_c$ is not too large ($\sim 5$ K) could be observed experimentally (here we assume singlet pairing). Note that in order to observe the cascade when $t_c \sim 5$ K, a very clean sample ($1/\tau < 100$ mK) is necessary as discussed in Sec. II. The second opinion is that $t_b$ and $t_c$ are strongly reduced due to 1D fluctuations according to[21,22]

$$\tilde{t}_b \sim \frac{t_b}{\pi}\left(\frac{t_b}{E_F}\right)^{\frac{\alpha}{1-\alpha}},$$
$$\tilde{t}_c \sim \frac{t_c}{\pi}\left(\frac{t_b}{E_F}\right)^{\frac{\alpha}{1-\alpha}}, \qquad (60)$$

where $E_F$ is the Fermi energy and $\alpha$ a coefficient which depends on the interaction constants. Using the estimations of Bourbonnais *et al.* obtained from the NMR relaxation rate,[39] $\tilde{t}_b \sim 30$ K, we obtain $\tilde{t}_c$=0.5–1.5 K (i.e., $\tilde{t}_z$=1–3 K). This value is close to the Josephson limit ($\tilde{t}_z \sim T_c$) and we expect in this case a slow decrease of $T_c(H)$ at high magnetic field as shown on Fig. 3 (long-dashed lines).

## VI. QUASI-2D SUPERCONDUCTORS

In the preceding considerations (Secs. II, III, and IV), the anisotropy of the $(x, y)$ planes does not seem to play a crucial role so that we may wonder whether a quasi-2D superconductor at high parallel magnetic field will present a similar phase diagram. An answer to this question can be given from semiclassical arguments. Consider a set of weakly coupled superconducting planes described by the dispersion law:

$$E(\mathbf{k}) = v(k_{\|} - k_F) + t_z \cos(k_z c), \qquad (61)$$

where $v$ is the Fermi velocity for the motion in the $(x, y)$ planes, $c$ the distance between planes, and $k_{\|} = |\mathbf{k}_{\|}|$

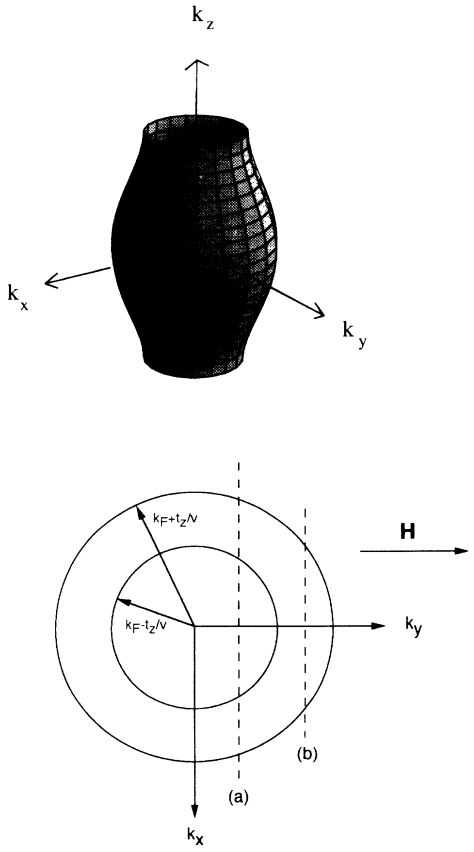


FIG. 11. Fermi surface of a quasi-2D conductor and its projection in the $(k_x, k_y)$ plane. The semiclassical orbits in reciprocal space are obtained by taking the intersection between the Fermi surface and the planes perpendicular to the magnetic field. These orbits can be open (a) or closed (b).

$[\mathbf{k}_{\|} = (k_x, k_y)]$. The coupling $t_z$ between planes is assumed to be much smaller than the Fermi energy so that the Fermi surface is open in the $k_z$ direction. The semiclassical orbits $\mathbf{k}(t)$ in reciprocal space are obtained by taking the intersection between the Fermi surface and the planes perpendicular to the magnetic field. For a field $\mathbf{H}(0, H, 0)$ parallel to the $y$ axis, these orbits can be either open or closed (Fig. 11). Elementary geometric considerations show that the amplitudes are between $2t_z/v$ and $2\sqrt{t_z t_{\|}}/v$ for the open orbits, and between 0 and $2\sqrt{t_z t_{\|}}/v$ for the closed orbits. Here $t_{\|} \sim vk_F$ is the hopping integral in the $(x, y)$ plane. It follows that the amplitudes of the real space orbits $\mathbf{r}(t)$ are between $2ct_z/\omega_c$ and $2c\sqrt{t_z t_{\|}}/\omega_c$ for the open orbits, and between 0 and $2c\sqrt{t_z t_{\|}}/\omega_c$ for the closed orbits, where $\omega_c = eHcv$. Since all the orbits are localized in the $z$ direction, the one-particle Green's function will be localized in this direction[40]. The presence of open orbits in the $x$ direction ensures that the electrons are not localized in this direction. The behaviors of the Green's functions in quasi-1D and quasi-2D conductors are then very similar. In particular, the particles will have a 2D motion confined in the $(x, y)$ planes at very high magnetic field $\omega_c \gg t_z$.[41] As long as only orbital effects are considered, there will be a strong reentrance of the superconducting phase. We expect that the system will evolve from the GL regime to this reentrant phase through a cascade of first-order transitions due to commensurability effects between the crystalline lattice spacing and the periodicity of the order parameter, as it is the case in a quasi-1D superconductor.

Although orbital effects of the field are similar in quasi-1D and quasi-2D systems, these two kinds of systems differ concerning the effect of Pauli pair-breaking. With the dispersion law (61), it is not possible to construct a LOFF state which would compensate significantly the Pauli pair-breaking effect as it is the case for the quasi-1D dispersion law (1). Except in very special cases [i.e., when $E(\mathbf{k}_{\|}) + \mu_B H = E(\mathbf{q}_{\|} - \mathbf{k}_{\|}) - \mu_B H$ on a significant part of the Fermi surface], the superconducting phase will be destroyed for a field of the order of the Pauli limited field. Therefore, the observation of quantum effects will be possible only near $H_{c2}^{(\mathrm{eik})}(0)$ and in superconducting materials which are not Pauli limited.

The possibility to observe quantum effects in quasi-2D superconductors certainly enlarges the number of materials which could exhibit high-field superconductivity. It should be remembered that these materials have to be clean and sufficiently anisotropic as discussed in Sec. II. Moreover, a too high zero-field critical temperature (like, for example, in high-$T_c$ superconductors) would be a drawback because the quantum effects would then appear at very high field. The quasi-2D organic superconductor $\beta$-(BEDT-TTF)$_2$I$_3$ in the high-$T_c$ ($\beta$-$H$) phase ($T_c \sim 10$ K) (Ref. 42) appears as a possible candidate for high-field superconductivity. This material has a coupling between planes $t_c = t_z/2 \sim 6$ K,[43] which corresponds to the Josephson limit depicted in Fig. 3. Because of its high purity,[43] impurity scattering should be inefficient in these materials. The low-$T_c$ ($\beta$-$L$) phase ($T_c \sim 1.3$ K) also appears very attractive, since the cascade is expected to be seen with such a low critical temperature. Unfortunately, the purity in this phase is not as high as in the $\beta$-$H$ phase[44] so that impurity scattering will certainly destroy the superconducting phase at high magnetic field. Let us also mention the case of artificial structures made of superconducting layers alternating with insulating layers.[45] The possibility to choose the ratio $t_z/T_c$ by varying the widths of the insulating layers could make these artificial structures candidates for high-field superconductivity, although the rather bad purity of these materials could be a serious limitation.

## VII. CONCLUSION

We have shown that in quasi-1D and quasi-2D superconductors, the quantum effects of the field lead to an unusual behavior at high magnetic field. Because of a magnetic-field-induced confinement of the electrons, superconductivity can survive at a high magnetic field contrary to the predictions of the GL theory. In the high-field regime, the superconducting state shows a kind of symmetry of a laminar type. We have shown that Pauli pair breaking and elastic scattering do not destroy this high-field superconductivity in clean materials with large anisotropy. A very important result is that the temperature and magnetic field scales are determined by the coupling between chains or planes. This means that the temperature and magnetic field ranges where high-field superconductivity is expected can be experimentally accessible if the appropriate material is chosen. Quasi-1D and quasi-2D organic superconductors have been proposed as possible candidates for the observation of superconductivity at high magnetic field.

The critical field $H_{c2}(T)$ in the $b'$ direction has been recently measured by Lee *et al.* in the Bechgaard salt (TMTSF)$_2$ClO$_4$.[46] An upward curvature in $H_{c2}(T)$ is observed below $T_c/2$ and down to $\sim$100 mK. We may wonder whether this unexpected curvature is a signature of the magnetic-field-induced dimensional crossover.

## ACKNOWLEDGMENTS

We thank C. Bourbonnais, D. Feinberg, D. Jérome, M. J. Naughton, and especially C. A. R. Sá de Melo for useful discussions. We also thank M. J. Naughton for sending us his experimental results prior to publication. This work was partially supported by NATO Grant No. 19189. The Laboratoire de Physique des Solides is Unité Associée au CNRS.

[1] L.P. Gor'kov, Zh. Eksp. Teor. Fiz. **36**, 1918 (1959) [Sov. Phys. JETP **9**, 1364 (1959)].
[2] A.A. Abrikosov, Zh. Eksp. Teor. Fiz. **32**, 1442 (1957) [Sov. Phys. JETP **5**, 1174 (1957)].
[3] See, for example, *Superconductivity*, edited by R.D. Parks (Dekker, New York, 1969).
[4] A.K. Rajagopal and R. Vasudevan, Phys. Lett. **23**, 539 (1966); L.W. Gruenberg and L. Gunther, Phys. Rev. **176**, 606 (1968).
[5] T. Maniv, R.S. Markiewicz, I.D. Wagner, and P. Wyder, Phys. Rev. B **45**, 13084 (1992); M.J. Stephen, *ibid.* **45**, 5481 (1992).
[6] J.E. Graebner and M. Robbins, Phys. Rev. Lett. **36**, 422 (1976).
[7] Z. Tešanović, M. Rasolt, and L. Xing, Phys. Rev. Lett. **63**, 2425 (1989); for a review see M. Rasolt and Z. Tešanović, Rev. Mod. Phys. **64**, 709 (1992).
[8] See also M.R. Norman, H. Akera, and A.H. MacDonald, in *Physical Phenomena in High Magnetic Fields*, edited by E. Manousakis *et al.* (Addison-Wesley, Reading, MA, 1992); A.K. Rajagopal, in *Selected Topics in Superconductivity*, edited by L.C. Gupta and M.S. Multani, Frontiers in Solid State Sciences Vol. 1 (World Scientific, Singapore, 1993).
[9] It should be noted that some authors have expressed strong doubts concerning the reality of reentrant superconductivity: C.T. Rieck, K. Sharnberg, and R.A. Klemm, Physica C **170**, 195 (1990); K. Sharnberg and C.T. Rieck, Phys. Rev. Lett. **66**, 841 (1991); V.M. Yakovenko, Phys. Rev. B **47**, 8851 (1993).
[10] K.B. Efetov, J. Phys. (Paris) Lett. **44**, L369 (1983).
[11] L.P. Gor'kov and A.G. Lebed', J. Phys. (Paris) Lett. **45**, L433 (1984).
[12] See review articles and references therein in *The Physics and Chemistry of Organic Superconductors*, edited by G. Saito and S. Kagoshima (Springer-Verlag, Berlin, 1987).
[13] A.G. Lebed', Pis'ma Zh. Eksp. Teor. Fiz. **44**, 89 (1986) [JETP Lett. **44**, 114 (1986)]; L.I. Burlachkov, L.P. Gor'kov, and A.G. Lebed', Europhys. Lett. **4**, 941 (1987).
[14] N. Dupuis, G. Montambaux, and C.A.R. Sá de Melo, Phys. Rev. Lett. **70**, 2613 (1993).
[15] P. Fulde and R.A. Ferrell, Phys. Rev. **135**, A550 (1964); A.I. Larkin and Yu.N. Ovchinnikov, Zh. Eksp. Teor. Fiz. **47**, 1136 (1964) [Sov. Phys. JETP **20**, 762 (1965)].
[16] B.S. Shandrasekhar, Appl. Phys. Lett. **1**, 7 (1962); A.M. Clogston, Phys. Rev. Lett. **9**, 266 (1962).
[17] See, for example, L.N. Bulaevskii, Int. J. Mod. B **4**, 1849 (1990).
[18] W.E. Lawrence and S. Doniach, in *Proceedings of the 12th International Conference on Low Temperature Physics LT12*, Kyoto, edited by E. Kanada (Academic, New York, 1970).
[19] V.M. Yakovenko, Zh. Eksp. Teor. Fiz. **93**, 627 (1987) [Sov. Phys. JETP **66**, 355 (1987)].
[20] N. Dupuis and G. Montambaux, Phys. Rev. B **46**, 9603 (1992).
[21] For a detailed discussion of 1D fluctuations and in particular of the meaning of "weak coupling limit," see C. Bourbonnais and L. Caron, Int. J. Mod. Phys. B **5**, 1033 (1991).
[22] C. Bourbonnais, in *Highly Correlated Fermions Systems and High-$T_c$ Superconductors*, Proceedings of Ecole d'Eté de Physique Théorique (Les Houches), edited by B. Doucot and R. Rammal (Elsevier, New York, 1991).
[23] The derivation of (12) from (11) is similar to the derivation of the Lawrence-Doniach model from the BCS theory in the case of weakly coupled planes: see L.N. Bulaevskii, Z. Eksp. Teor. Fiz. **64**, 2241 (1973) [Sov. Phys. JETP **37**, 1133 (1973)].
[24] For a description of the Bechgaard salts in Ginzburg-Landau theory, see L.P. Gorkov and D. Jérome, J. Phys. (Paris) Lett. **46**, L643 (1985).
[25] See, for instance, J. Sólyom, Adv. Phys. **28**, 201 (1979).
[26] L.P. Gor'kov, Zh. Eksp. Teor. Fiz. **37**, 1407 (1960) [Sov. Phys. JETP **10**, 998 (1960)].
[27] The details of this calculation will be published elsewhere.
[28] P.W. Anderson, J. Phys. Chem. Solids **11**, 26 (1959).
[29] See, for instance, J.P. Carton, J. Phys. I **1**, 113 (1991).
[30] K.B. Efetov, Zh. Eksp. Teor. Fiz. **76**, 1781 (1979) [Sov. Phys. JETP **49**, 905 (1979)].
[31] A. Buzdin and D. Feinberg, J. Phys. France **51**, 1971 (1990).
[32] N. Dupuis, Ph.D thesis, Université Paris-Sud, 1993.
[33] W. Kang, S.T. Hannahs, and P.M. Chaikin, Phys. Rev. Lett. **70**, 3091 (1993).
[34] D. Jérome and H.J. Schulz, Adv. Phys. **31**, 299 (1982).
[35] V.J. Emery, Synth. Met. **13**, 21 (1986); M.T. Béal-Monod, C. Bourbonnais, and V.J. Emery, Phys. Rev. B **34**, 7716 (1984).
[36] C. Bourbonnais and L. Caron, Europhys. Lett. **5**, 209 (1988).
[37] A different opinion has been proposed by Yakovenko. Assuming that superconductivity is due to an effective attractive intrachain interaction, this author showed that a SDW can be stabilized under magnetic field as it is observed experimentally in the Bechgaard salts (Ref. 19).
[38] R.L. Greene, P. Haen, S.Z. Huang, E.M. Engler, M.Y. Choi, and P.M. Chaikin, Mol. Cryst. Liq. Cryst. **79**, 183 (1982); K. Murata, M. Tokumoto, H. Anzai, K. Kajimura, and T. Ishiguro, Jpn. J. Appl. Phys. **26**, BI04 (1987).
[39] C. Bourbonnais, F. Creuzet, D. Jérome, K. Bechgaard, and A. Moradpour, J. Phys. (Paris) Lett. **45**, L755 (1984).
[40] Here we use the fact that the semiclassical orbits can be obtained from the one-particle Green's function by using a saddle point approximation.
[41] All the orbits will be 2D only if $\omega_c \gg \sqrt{t_\parallel t_z}$. Nevertheless, the weight of the closed orbits is weak and the amplitude of the orbits will be of the order of $c(t_z/\omega_c)$ after averaging over the Fermi surface.
[42] V.N. Laukhin, E.E. Kostyuchenko, Yu.V. Sushko, I.F. Shegolev, and E.B. Yagunskii, Pis'ma Zh. Eksp. Teor. Fiz. **41**, 68 (1985) [JETP Lett. **41**, 81 (1985)]; K. Murata, M. Tokumoto, H. Anzai, H. Bando, G. Saito, K. Kajimura, and T. Ishiguro, J. Phys. Soc. Jpn. **54**, 1236 (1985); F. Creuzet, G. Creuzet, D. Jérome, D. Schweitzer, and H.J. Keller, J. Phys. Lett. (Paris) **46**, L1079 (1985).
[43] W. Kang, G. Montambaux, J.R. Cooper, D. Jérome, P. Batail, and C. Lenoir, Phys. Rev. Lett. **62**, 2559 (1989).
[44] N. Toyata *et al.*, J. Phys. Soc. Jpn. **57**, 2616 (1988).
[45] See, for instance, S.T. Ruggiero and M.R. Beasley, in *Synthetic Modulated Structures*, edited by L.L. Chang and B.C. Giessen (Academic, New York, 1985).
[46] I.J. Lee, A.P. Hope, M. Chaparala, and M.J. Naughton (unpublished).

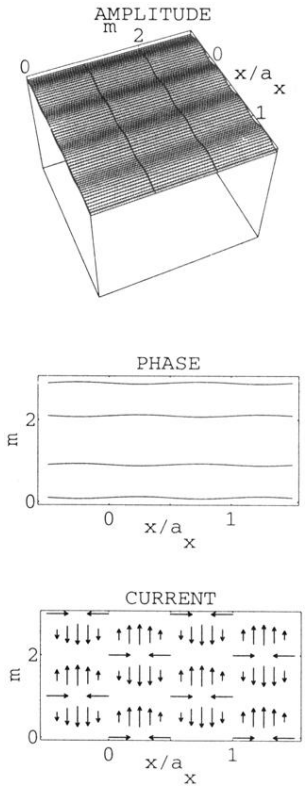


FIG. 10. Phase $Q = 0$, $N = 2$ ($H = 5.8$ T).

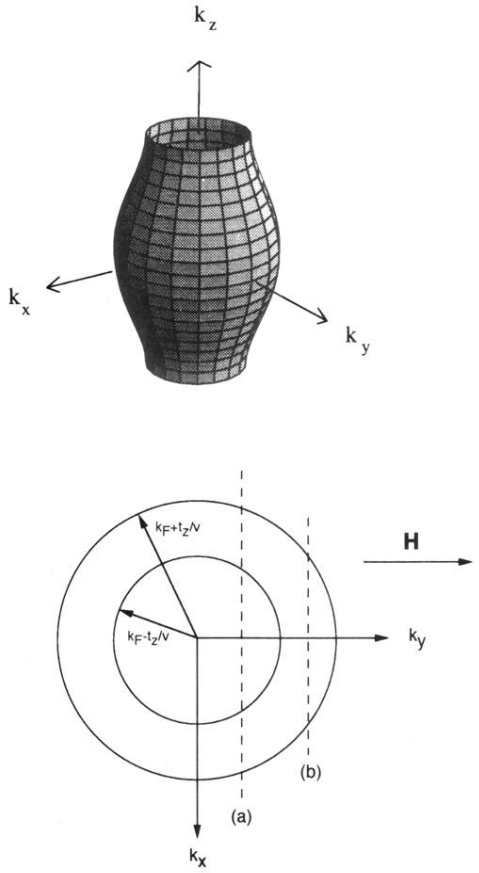


FIG. 11. Fermi surface of a quasi-2D conductor and its projection in the $(k_x, k_y)$ plane. The semiclassical orbits in reciprocal space are obtained by taking the intersection between the Fermi surface and the planes perpendicular to the magnetic field. These orbits can be open (a) or closed (b).

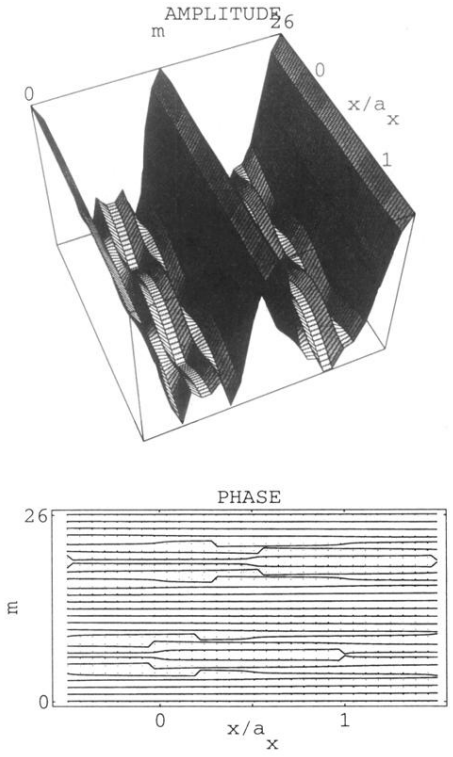


FIG. 7. Phase $Q = 0$, $N = 26$ ($H = 0.48$ T).

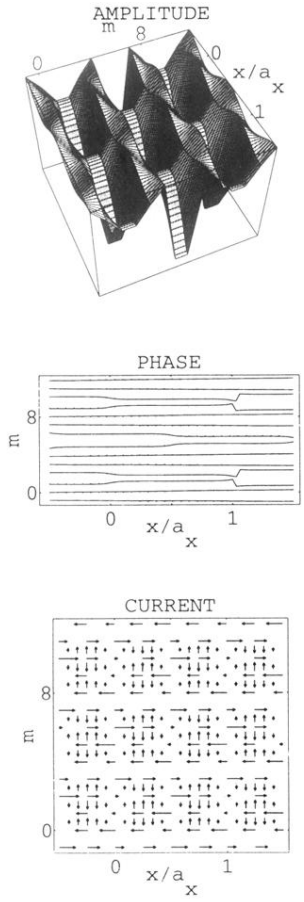


FIG. 8. Phase $Q = G$, $N = 8$ ($H = 1.7$ T).

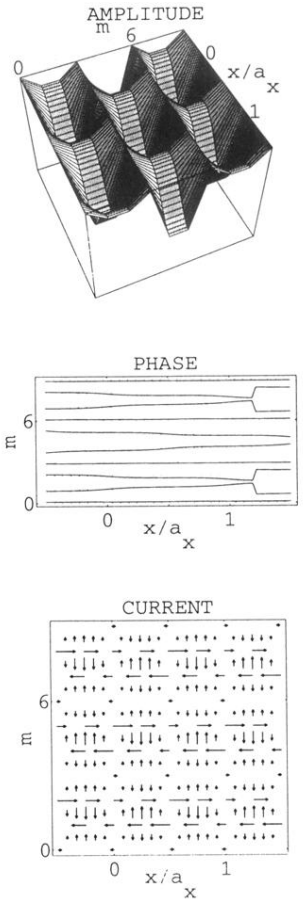


FIG. 9. Phase $Q = 0$, $N = 6$ ($H = 2.4$ T).